Reactivity of Superoxide Radical Anion and Hydroperoxyl Radical with α-Phenyl-*N*-*tert*-butylnitrone (PBN) Derivatives

Grégory Durand,*,† Fanny Choteau,† Bernard Pucci,† and Frederick A. Villamena*,‡

Laboratoire de Chimie Bioorganique et des Systèmes Moléculaires Vectoriels, Université d'Avignon et des Pays de Vaucluse, Faculté des Sciences, 33 rue Louis Pasteur, 84000 Avignon, France, and Department of Pharmacology and Davis Heart and Lung Research Institute, The Ohio State University, Columbus, Ohio 43210

Received: June 4, 2008; Revised Manuscript Received: August 26, 2008

Nitrones have exhibited pharmacological activity against radical-mediated pathophysiological conditions and as analytical reagents for the identification of transient radical species by electron paramagnetic resonance (EPR) spectroscopy. In this work, competitive spin trapping, stopped-flow kinetics, and density functional theory (DFT) were employed to assess and predict the reactivity of $O_2^{\bullet-}$ and $HO_2^{\bullet}$ with various para-substituted α-phenyl-*N*-*tert*-butylnitrone (PBN) spin traps. Rate constants of $O_2^{\bullet-}$ trapping by nitrones were determined using competitive UV−vis stopped-flow method with phenol red (PR) as probe, while $HO_2^{\bullet}$ trapping rate constants were calculated using competition kinetics with 5,5-dimethylpyrroline *N*-oxide (DMPO) by employing EPR spectroscopy. The effects of the para substitution on the charge density of the nitronyl-carbon and on the free energies of nitrone reactivity with $O_2^{\bullet-}$ and $HO_2^{\bullet}$ were computationally rationalized at the PCM/B3LYP/6-31+G(d,p)//B3LYP/6-31G(d) level of theory. Theoretical and experimental data show that the rate of $O_2^{\bullet-}$ addition to PBN derivatives is not affected by the polar effect of the substituents. However, the reactivity of $HO_2^{\bullet}$ follows the Hammett equation and is increased as the substituent becomes more electron withdrawing. This supports the conclusion that the nature of $HO_2^{\bullet}$ addition to PBN derivatives is electrophilic, while the addition of $O_2^{\bullet-}$ to PBN-type compounds is only weakly electrophilic.

I. Introduction

For several decades, nitrones have been extensively used in spin trapping[1] due to their ability to identify a variety of biologically relevant free radicals such as oxygen-centered radicals, e.g., hydroxyl radical ($HO^{\bullet}$), superoxide radical anion ($O_2^{\bullet-}$), and alkoxyl radical ($RO^{\bullet}$), as well as C-centered and S-centered radicals such as methyl ($^{\bullet}CH_3$) and thiyl ($RS^{\bullet}$). Spin trapping involves addition of a free radical to nitrone yielding a persistent aminoxyl spin adduct which can be detected and characterized by electron paramagnetic resonance (EPR) spectroscopy. α-Phenyl-*N*-*tert*-butylnitrone (PBN) and 5,5-dimethyl-1-pyrrolidine *N*-oxide (DMPO) (Figure 1) have been the most commonly used spin traps, but DMPO and its derivatives have shown better properties than PBN-type nitrones due to longer half-lives and distinctive EPR spectra of their radical adducts. The half-lives of the $HO_2^{\bullet}$ adducts[2] of PBN and DMPO in water are short with $t_{1/2} < 1$ min but are longer in organic solvents such as dimethylformamide (DMF) and pyridine with $t_{1/2}$ of ∼4 min and ∼8 min, respectively.[3] However, nitrones have some limitations such as bioreducibility of their spin adducts, low rate of reactivity to $O_2^{\bullet-}$, and low accumulation in the sites of radical production. To overcome such limitations, new spin traps such as 5-diethoxyphosphoryl-5-methylpyrroline *N*-oxide (DEPMPO), *N*-benzyliene-1-diethoxyphosphoryl-1-methylethylamine *N*-oxide (PPN), 5-(cholesteryloxyethoxyphosphoryl)-5-methylpyrroline *N*-oxide (5-ChEPMO), [4-[4-[[(1,1-dimethylethyl)oxidoimino]methyl]phenoxy]butyl]triphenylphosphonium bromide (MitoPBN), and *N*-[4-(lactobionamidomethylene)benzylidene]-*N*-[1,1-dimethyl-2-(*N*-octanoyl)amido]ethylamine *N*-oxide (LPBNAH) (Figure 1) have been developed with improved spin trapping properties[4,5] and cell permeability.[6−9]

Among the free radicals that are produced by aerobic organisms, $O_2^{\bullet-}$ has attracted considerable attention due to the crucial role it plays in the modulation of cellular function and the havoc it creates in unregulated concentration.[10,11] Intrinsically, $O_2^{\bullet-}$ is a relatively weak oxidant (or reductant), as demonstrated by its limited reactivity toward lipids, nucleotides, amino acids, and sugars. In spite of the limited reactivity of $O_2^{\bullet-}$, it is a major source of highly reactive species known to be generated in biological systems such as $ONOO^-$, HOCl, $GSSG^{\bullet-}$, and $CO_3^{\bullet-}$.[10] The ability of $O_2^{\bullet-}$ to chemically or enzymatically self-dismutate to H_2O_2 and subsequently to $HO^{\bullet}$ via the Fenton reaction and also its selective reactivity toward transition metal ions account for $O_2^{\bullet-}$ high toxicity. Furthermore, the higher reactivity of $O_2^{\bullet-}$ at lower pH is due to the formation of hydroperoxyl radical ($HO_2^{\bullet}$) ($pK_a(HO_2^{\bullet}/O_2^{\bullet-}) = 4.8$), which is more reactive than $O_2^{\bullet-}$. Due to the crucial role of $O_2^{\bullet-}$ and $HO_2^{\bullet}$ in the initiation of oxidative damage to biomolecules, it is imperative to explore the specific molecular and cellular pathways of free-radical production associated with the pathogenesis of some diseases.

Paradoxically, despite the poor reactivity of PBN and DMPO to $O_2^{\bullet-}$, they have been widely used as protective agents in several biological models of oxidative stress.[12] Although the rate constants for the spin trapping of $HO^{\bullet}$ by PBN and DMPO are in the same range, i.e., $(2.7-3.6) \times 10^9$ and $(6.1-8.5) \times 10^9$ M^{-1} s^{-1}, respectively,[2] the rate of $O_2^{\bullet-}$ trapping ranges only from 1.2 to 310 M^{-1} s^{-1} for DMPO[2,13] and ∼18 M^{-1} s^{-1} for

* To whom correspondence should be addressed. Phone: +33 4 9014-4445 (G.D.); (614) 292-8215 (F.V.). Fax: + 33 4 9014-4441 (G.D.); (614) 688-0999 (F.V.). E-mail: gregory.durand@univ-avignon.fr (G.D.); frederick.villamena@osumc.edu (F.V.).

† Université d'Avignon et des Pays de Vaucluse.

‡ The Ohio State University.

10.1021/jp804929d CCC: $40.75
Published on Web 11/11/2008

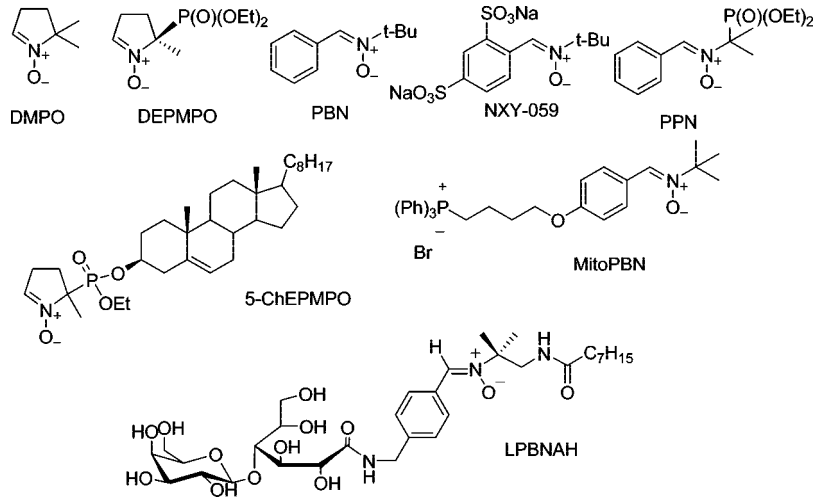

Figure 1. Chemical structures of linear and cyclic nitrones.

PBN.[14] The nitrone PBN has exhibited a variety of pharmacological activities. For example, Novelli et al.[15] showed that preadministration of PBN protects rats from endotoxic shock and showed broad neuroprotective activity.[16,17] Moreover, the ability of PBN to prevent doxorubicin cardiotoxicity[18] or thalidomide-induced birth defects[19] has been reported. However, despite the exceptional potency of PBN in the prevention of some pathophysiological conditions, the molecular mechanism of its action remains obscure.[20,21] The spin trap disodium [(*tert*-butylimino)methyl]benzene-1,3-disulfonate *N*-oxide (NXY-059) is the first neuroprotective agent to reach phase 3 clinical trials in the USA.[22] It is believed that the free radical trapping properties of NXY-059 are the basis of its neuroprotective action; however, experimental evidence suggests the possibility of other mechanisms being involved. In contrast to PBN, only a few studies on the pharmacological properties of DMPO have been reported.[23] There is therefore a need to better understand the chemical properties of nitrones in order to facilitate their development for analytical and therapeutic applications.

One of the promising strategies in the design of novel spin traps is to selectively target these compounds in relevant sites of radical production, mainly the mitochondrial electron transport chain and the membrane-bound NAD(P)H oxidase.[6,24,25] With the expectation that amphiphilic compounds possessing both hydrophilic and lipophilic groups would exhibit improved bioavailability, a novel class of amphiphilic nitrones has been recently developed.[8,9,26,27] Selective targeting is usually achieved by conjugating the nitrones to target-specific ligands. In addition to the type of ligands that are tethered to nitrones, it has been demonstrated that the nature of the linker group also affects its bioactivity.[27] Therefore, the nature of the linker group, target specificity, and efficiency of radical trapping must be considered in the design of new spin traps with improved properties.

In this work, two new para amido-substituted PBNs were synthesized along with dimethyl amino, methoxy, carboxylic acid, and cyano para-substituted PBN compounds. The relative rate constants of hydroperoxyl adduct formation from PBN derivatives were experimentally determined by competition kinetics using EPR and stopped-flow techniques. The correlation between the polar effect of the substituents and the experimental rate constants for the formation of hydroperoxyl adduct was also investigated. The electronic properties of the nitrones and their respective spin adducts were calculated at the PCM/B3LYP/6-31+G(d,p)//B3LYP/6-31G(d) level of theory.

II. Experimental Section

A. Synthesis. All starting materials were purchased and used without further purification. All solvents were distilled and dried according to standard procedures. TLC analyses were performed on sheets precoated with silica gel 60F254. The progress of reaction was monitored by exposure of the TLC to UV light (254 nm) and by using 5% sulfuric acid solution in methanol or 5% ninhydrin solution in ethanol as visualizing agents, and then heating at 150 °C. Flash chromatography was carried out on Merck silica gel Geduran Si 60 (0.063−0.200 mm). Mass spectra were recorded on a Triple quadripolar spectrometer API III Plus Sciex for ESI+. Melting points were measured on an Electrothermal IA9100 apparatus and have not been corrected. UV spectra were recorded on a Varian Cary 100. The ^{1}H and ^{13}C NMR spectra were recorded on a Brüker AC-250 spectrometer. Chemical shifts are given in parts per million (ppm) relative to tetramethylsilane using the deuterium signal of the solvent ($CDCl_3$ or DMSO-d_6) as heteronuclear reference. Abbreviations used for signal patterns are the following: s, singlet; d, doublet; t, triplet; q, quartet; m, multiplet. A concentration of 300 mM in DMSO-d_6 was used in the Hammett correlation, and 2% $CHCl_3$ was added to the NMR tube as internal reference.

N-tert-Butyl-α-(4-methylbenzamide)phenylnitrone (5). At 0 °C in a sealed tube, *N-tert*-butyl-α-(4-(2,5-dioxopyrrolidin-1-yl)ester)phenylnitrone[27] (0.70 g, 2.2×10^{-3} mol, 1 equiv) was dissolved in THF under argon atmosphere. Methylamine chloride (0.178 g, 2.64×10^{-3} mol, 1.2 equiv) was suspended under stirring, and triethylamine (TEA) was added dropwise until complete dissolution of the salts (pH 8−9). The mixture was stirred at 40 °C for 48 h, then filtered, and concentrated in vacuo. Purification of the resulting crude compound by flash chromatography eluting with EtOAc/MeOH (9:1 v/v) followed by recrystallization from EtOAc afforded **5** (0.250 g, 1.07×10^{-3} mol, 48% yield) as white needles. R_f 0.38 in EtOAc/MeOH (9:1 v/v). mp 167.6−168.6 °C. ^{1}H NMR ($CDCl_3$, 250 MHz) δ 8.35 (2H, d, $J = 8.5$ Hz), 7.83 (2H, d, $J = 8.6$ Hz), 7.62 (1H, s), 6.42 (1H, s), 3.04 (3H, d, $J = 4.85$ Hz), 1.63 (9H, s). ^{13}C NMR ($CDCl_3$, 62.86 MHz) δ 167.5, 135.4, 133.6, 129.2, 128.7, 127.0, 71.4, 28.3, 26.9. λ_{max} (CH_2Cl_2) 316 nm. HRMS (ESI+) Calcd for $C_{13}H_{19}N_2O_2$ $[M + H]^+$: 235.1441. Found: 235.1441.

N-tert-Butyl-α-(4-benzylacetamide)phenylnitrone (9). (4-(1,3-Dioxolan-2-yl)phenyl)methanamine[28] (1.5 g, 8.37×10^{-3} mol) was dissolved in a pyridine/Ac_2O (1:1 v/v) mixture at 0

°C. After 14 h of being stirred at room temperature, the solution was poured into cold water and extracted with EtOAc (3×). The organic layer was washed with brine (2×), dried over Na_2SO_4, and concentrated in vacuo. The resulting yellow oil (1.2 g, 5.42×10^{-3} mol) was dissolved in a AcOH/H_2O (1:1 v/v) mixture and stirred at room temperature for 20 h. The solvent was removed in vacuo, and residual traces of water were removed by azeotropic distillation with toluene. Purification of the resulting crude powder by recrystallization from EtOAc/*n*-hexane afforded *N*-(4-formylbenzyl)acetamide (0.600 g, 3.38×10^{-3} mol, 40% yield from 4-(1,3-dioxolan-2-yl)phenyl-)methanamine[28]) as a white powder. ^{1}H NMR ($CDCl_3$, 250 MHz) δ 10.00 (1H, s), 7.86 (2H, d, $J = 8.1$ Hz), 7.45 (2H, d, $J = 8.0$ Hz), 6.09 (1H, bs), 4.53 (2H, d, $J = 6.0$ Hz), 2.08 (3H, s). ^{13}C NMR ($CDCl_3$, 62.86 MHz) δ 191.8, 170.2, 145.4, 135.7, 130.1, 128.1, 43.3, 23.2. *N*-(4-Formylbenzyl)acetamide (0.600 g, 3.38×10^{-3} mol, 1 equiv) and *N-tert*-butylhydroxylamine acetate (0.585 g, 3.92×10^{-3} mol, 1.15 equiv) were dissolved in toluene in the presence of a catalytic amount of *p*-toluenesulfonic acid. After 3 h of reflux, a small portion of hydroxylamine (0.150 g, 1×10^{-3} mol, 0.3 equiv) was added and the mixture was refluxed again for 4 h. The solvent was evaporated in vacuo, and the resulting oil was dissolved in CH_2Cl_2. The organic layer was washed with $NaHCO_3$ (2×) and brine (2×), dried over Na_2SO_4, and then evaporated. Purification of the resulting crude powder by recrystallization from EtOAc/*n*-hexane afforded **9** (0.50 g, 2.0×10^{-3} mol, 60% yield) as white needles. R_f 0.30 in EtOAc/MeOH (9:1 v/v). mp 171.2−172.6 °C. ^{1}H NMR ($CDCl_3$, 250 MHz) δ 8.35 (1H, m), 8.31 (2H, d, $J = 8.1$ Hz), 7.82 (1H, s), 7.29 (2H, d, $J = 8.1$ Hz), 4.29 (2H, d, $J = 5.9$ Hz), 1.90 (3H, s), 1.59 (9H, s). ^{13}C NMR ($CDCl_3$, 62.86 MHz) δ 169.7, 141.6, 130.6, 128.9, 128.8, 129.7, 127.3, 70.7, 42.4, 28.4, 23.0. λ_{max} (CH_2Cl_2) 302 nm. HRMS (ESI+) Calcd for $C_{14}H_{21}N_2O_2$ $[M + H]^+$: 249.1597. Found: 249.1598.

B. EPR Measurements. EPR measurements were carried out on a Bruker EMX-X band with an HS resonator at room temperature. General instrument settings were as follows: microwave power, 10 mW; microwave frequency, 9.87 GHz; modulation amplitude, 1.0 G; receiver gain, $(8.93-10.00) \times 10^4$; sweep width, 100 G; time constant, 20.48 ms; sweep time, 40.96 s. General instrument settings for kinetic experiments were as follows: microwave power, 10 mW; microwave frequency, 9.87 GHz; modulation amplitude, 1.0 G; receiver gain, 1.00×10^5 (except for compound **4**, 1.00×10^4); sweep width, 0 G; time constant, 1310.72 ms; sweep time, 2048 s. Measurements were performed using 50 μL capillary tubes. Simulations were carried out using the EPR Software WinSim2002.[29]

C. Competitive Spin Trapping. All kinetic experiments were performed using a pyridine solution of H_2O_2 (160 mM). In a typical competitive spin-trapping experiment, a 75 μL pyridine solution contained 100 mM PBN derivatives, 160 mM H_2O_2, and varying amounts of DMPO (0−50 mM). The solutions were transferred into 50 μL capillary tubes, and kinetic measurements were initiated 42 s after the addition of hydrogen peroxide solution. The growth of the second low-field peak was monitored by EPR as a function of time over a period of 60 s. All the data were the average of at least two measurements.

D. Stopped-Flow Kinetics. The procedure was similar to the procedure described by Villamena et al.[13] Briefly, a solution of KO_2 was prepared by vigorously mixing ~200 mg of KO_2 in ~5 mL of DMF. After 10 min, 1 mL of the supernatant was further diluted to ~12−15 mL in order to reach a maximum of absorbance of ~1 at 575 nm when mixed with 500 μM phenol red solution in 90% DMF−10% H_2O. The diluted solution was tightly covered and kept in ice during the course of the experiment. A slight decrease of superoxide concentration was observed during the first 5 min of standing, after which the concentration remained constant for at least 1 h. Therefore, measurements were initiated 10 min after dilution. Solutions of the nitrones and 500 μM phenol red in 90% DMF−10% H_2O solution were prepared prior to the experiment. Stopped-flow reactions were initiated by mixing 150 μL of dilute KO_2 solution and 150 μL of nitrones solution, and the growth of the transient absorption at 575 nm was monitored using a Varian Cary 50 Bio UV−vis spectrophotometer equipped with an RX 2000 Rapid Mix accessory from Applied Photophysics. The plot was linear during the first 6−8 s, and the data were fitted to a linear equation ($y = ax + b$). The absence of any absorbance at 575 nm due to the nitrones was verified by scanning a 75 mM solution of pure nitrones in 95% DMF−5% H_2O.

E. Computational Methods. Density functional theory (DFT)[30] was applied in this study to determine the optimized geometries, vibrational frequencies, and single-point energies of all stationary points.[31,32] The effect of aqueous solvation was also investigated using the polarizable continuum model (PCM).[33] All calculations were performed using Gaussian 03[34] at the Ohio Supercomputer Center. Single-point energies were obtained at the B3LYP/6-31+G** level based on the optimized B3LYP/6-31G* geometries. Charge and spin densities were obtained from a natural population analysis (NPA)[35] at the single-point PCM/B3LYP/6-31+G**//B3LYP/6-31G* level. These calculations used six Cartesian d functions. Stationary points for nitrones and its respective adducts have zero imaginary vibrational frequency as derived from a vibrational frequency analysis (B3LYP/6-31G*). A scaling factor of 0.981 was used for the zero-point vibrational energy (ZPE) corrections for the B3LYP/6-31G* level.[36] Spin contamination for all of the stationary point of the radical structures was negligible, i.e., $\langle S^2 \rangle = 0.75$.

III. Results and Discussion

A. Synthesis. Commercially available benzaldehyde derivatives allow the facile synthesis of a series of para-substituted PBN derivatives. The condensation reaction of *N-tert*-butylhydroxylamine with the respective para-substituted benzaldehyde derivatives was employed for the synthesis of the nitrones[37] (Scheme 1). 4-Me_2N-PBN, 4-NC-PBN, and 4-MeO-PBN were synthesized through direct condensation of the appropriate benzaldehyde to the *N-tert*-butylhydroxylamine acetate in refluxing toluene by following the general procedure described by Hinton and Janzen.[37] 4-HO_2C-PBN was synthesized in glacial acetic acid at 60 °C in the presence of molecular sieves (4 Å). 4-MeNHCO-PBN was synthesized from activated PBN as a 4-*N*-hydroxysuccinimide derivative[27] and methylamine hydrochloride in the presence of triethylamine. The benzylamine derivative **6** was prepared from 4-cyanobenzaldehyde according to the published procedure.[28] Acetylation of compound **6** followed by removal of the dioxolane group in acidic condition led to *N*-(4-formylbenzyl)acetamide with 40% yield from compound **6**. Finally, *N*-(4-formylbenzyl)acetamide was reacted with *N-tert*-butylhydroxylamine acetate in toluene under inert condition, yielding 4-AcNHCH_2-PBN. All nitrones were carefully purified by flash chromatography and/or successive recrystallizations until no residual EPR signal was observed. The novel nitrones **5** and **9** were fully characterized by ^{1}H NMR, ^{13}C NMR, and mass spectrometry.

B. Hammett Constant Correlation with Calculated Charge Densities of the Nitrones and Hyperfine Splitting Constants of the Spin Adducts. The natural population analysis (NPA) charges on the nitronyl-carbon, nitronyl-nitrogen, and nitronyl-

SCHEME 1: Synthesis of PBN Derivatives[a]

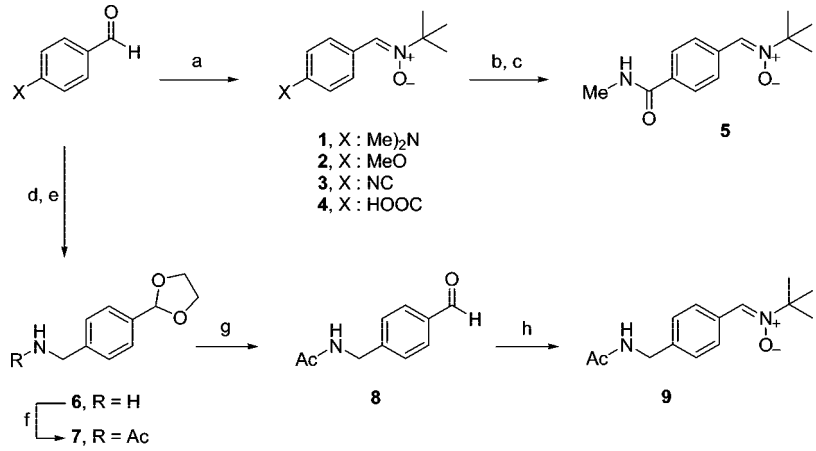

[a] Reagents and conditions: (a) *N-tert*-butylhydroxylamine acetate (1.3 equiv), *p*-TsOH, toluene for compounds **1**−**3** or *N-tert*-butylhydroxylamine acetate (1.3 equiv), molecular sieves (4 Å), AcOH for compound **4**; (b) compound **4**, HOSu (1.2 equiv), DCC (1.2 equiv), CH_2Cl_2; (c) methylamine hydrochloride (1.2 equiv), TEA, THF, sealed tube; (d) 4-cyanobenzaldehyde, ethylene glycol (4 equiv), *p*-TsOH, toluene; (e) $LiAlH_4$ (2 equiv), THF; (f) Ac_2O/Pyr 1:1 (v/v); (g) AcOH/H_2O 1:1 (v/v); (h) *N-tert*-butylhydroxylamine acetate (1.3 equiv), *p*-TsOH, toluene.

TABLE 1: Hammett Sigma Para Constants (σ_p), Nitronyl Group Charge Densities (e), and Hyperfine Splitting Constants (hfsc's) of the Simulated $HO_2^{\bullet}$ Adducts Generated from Pyridine/H_2O_2 and DMF/KO_2 Systems

						hfsc's of $HO_2^{\bullet}$ adducts					
		charge densities[b] (e)				pyridine/H_2O_2			DMF/KO_2		
compound	σ_p[a]	C	N	O	H	a_N	$a_{\beta\text{-H}}$	$a_{\gamma\text{-H}}$	a_N	$a_{\beta\text{-H}}$	$a_{\gamma\text{-H}}$
4-Me_2N-PBN (**1**)	−0.83	0.015	0.053	−0.635	0.250	13.88	1.92	−	14.13	2.41	−
4-MeO-PBN (**2**)	−0.27	0.013	0.064	−0.619	0.252	13.71	1.72	−	14.41	2.11	−
4-NC-PBN (**3**)	0.66	−0.003	0.090	−0.577	0.258	13.30	1.37	−	14.26	1.92	−
4-HO_2C-PBN (**4**)	0.45	−0.001[c]	0.088[c]	−0.581[c]	0.257[c]	14.60	2.41	−	13.42	1.52	−
		0.000[d]	0.087[d]	−0.581[d]	0.257[d]						
4-MeNHCO-PBN (**5**)	0.36	0.002	0.082	−0.591	0.256	13.46	1.49	−	14.42	1.86	−
4-$AcNHCH_2$-PBN (**9**)	−0.05	0.009	0.073	−0.605	0.253	13.59	1.61	−	14.44	1.76	−
PBN	0	0.009	0.073	−0.606	0.253	13.54	1.61	−	14.51	1.76	−
DMPO[e]	−	0.019	0.067	−0.625	−	12.79[f]	10.19[f]	1.36[f]	12.80	10.10	1.40

[a] Data from Hansch et al.[38] [b] Determined from a natural population analysis (NPA) at the single-point PCM/B3LYP/6-31+G(d,p)//B3LYP/6-31G(d) level. [c] Trans conformation. [d] Cis conformation. [e] Data from Villamena et al.[13] [f] This work.

oxygen atoms were determined at the PCM/B3LYP/6-31+G(d,p)//B3LYP/6-31G(d) level (Table 1). A high degree of correlation between the charge densities of the nitronyl group atoms and the Hammett sigma para constants (σ_p) of the different substituents[38] can be observed (Figure 2), which confirms the presence of a polar effect from the substituents on the nitronyl charge density. The polar effect on the charge densities can be explained by the resonance structures shown in Scheme 2. Electron-donating substituents tend to increase positivity and negativity on the carbon and oxygen atoms, respectively, while the positivity on the nitrogen is decreased. This substituent effect is reversed in the presence of electron-withdrawing groups.

The effect of the nature of the substituent on the charge density of the nitrone moiety was further confirmed using ^{1}H NMR spectroscopy. Figure 3 shows the ^{1}H NMR chemical shifts of the β-hydrogen at 7.56−8.05 ppm which exhibited a downfield shift in the presence of an electron-withdrawing substituent, characteristic of deshielding of the methine proton due to the increased positive character of the nitronyl-hydrogen. However, correlation of the ^{13}C NMR chemical shift of the nitronyl-carbon was difficult due to the extensive overlap of the nitronyl-carbon chemical shift with that of the aromatic carbons. A DEPT 90 experiment was performed in order to clearly observe the CH but gave no significant correlation for the nitronyl-carbon chemical shifts with respect to the Hammett σ constants, similar to that observed for the carbonyl-carbon chemical shift using benzaldehyde derivatives.[39] The downfield shift of the nitronyl-carbon and β-hydrogen of DMPO at acidic pH was previously reported[40] and was due to the increased positive character of the nitronyl-carbon upon protonation of the oxygen atom. This study further demonstrates the effect of the nature of substituents on the charge densities in the nitrone moiety.

The EPR hyperfine splitting constants (hfsc's) of the simulated $HO_2^{\bullet}$ adducts are shown in Table 1. The observed hfsc's in DMF/water are higher than in pyridine, indicative of the solvent effect on the hyperfine splitting constants due perhaps to the conformational changes around the hydroperoxyl group and the phenyl substituent relative to the nitroxyl moiety. Since the magnitude of the hfsc's depends mostly on the degree of orbital overlap between the C−H_β σ-orbital and the singly occupied molecular orbital (SOMO) of the nitroxyl nitrogen,[41] it can be assumed that the negligible perturbation on the hfsc's for DMPO-O_2H in both solvents is due to a more hindered rotation along the $\angle$O−N−C−H_β dihedral angle compared to the linear nitrones in which the N−C bond along $\angle$O−N−C−H_β can freely rotate. In order to confirm whether the spectra obtained using the DMF/KO_2 system were not of $HO^{\bullet}$ adducts, $HO^{\bullet}$ adducts were independently generated in DMF using the Fenton reaction. Results show that, in general, the a_N and $a_{\beta\text{-H}}$ values were significantly lower for $HO^{\bullet}$ adducts compared to $HO_2^{\bullet}$

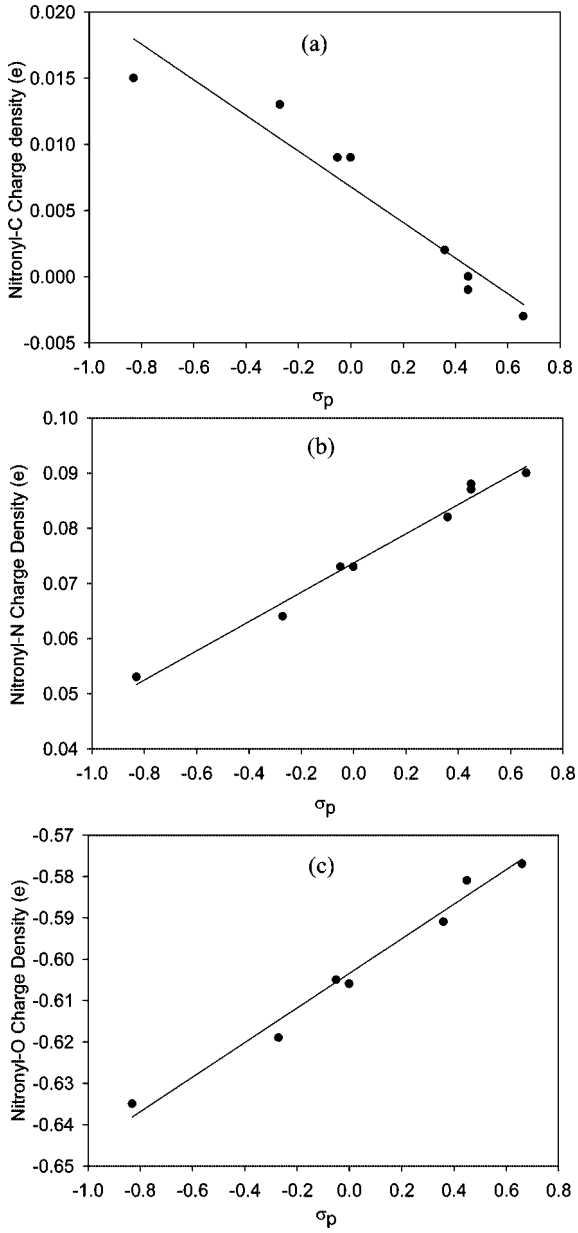

Figure 2. Correlation of σ_p values with the (a) nitronyl-carbon charge densities ($R^2 = 0.918$), (b) nitronyl-nitrogen charge densities ($R^2 = 0.984$), and (c) nitronyl-oxygen charge densities ($R^2 = 0.977$).

adducts in DMF, indicating that the species generated using KO_2/DMF are not those of $HO^\bullet$ adducts (see Table S1 in the Supporting Information). Although the half-life of PBN-O_2H in water is short ($t_{1/2} < 30$ s), it has been shown that PBN-O_2H is longer lived in pyridine and DMF with $t_{1/2} \sim 4$ min,[3] which further supports that the observed hfsc's were those of $HO_2^\bullet$ adducts within the measured kinetic time frame.

However, Table 2 shows no significant differences in the calculated hfsc's in the presence of the bulk dielectric effects of water, DMSO, and isoquinoline. Consideration of explicit solvent−spin adduct interaction along with the bulk dielectric effect of the solvent have been shown to give more accurately predicted hfsc's.[42] However, since explicit water interaction only has small effect on the predicted hfsc's, we only considered the bulk dielectric solvent effect, and this has been shown to predict reasonable hfsc values.[43] Significant correlations between the σ_p values of the different substituents[38] and the predicted hfsc's were observed (see Figures S1 and S2 in the Supporting Information). However, while R^2 values observed in the DMF/KO_2 system were 0.502 and 0.955 for the a_N or $a_{\beta\text{-H}}$ values, respectively, much higher correlations were observed in the pyridine/H_2O_2 system with R^2 of 0.983 and 0.997 for the nitrogen and hydrogen hfsc's, respectively. In pyridine, the electron-donating para-substituted spin adducts, 4-Me_2N-PBN/O_2H and 4-MeO-PBN/O_2H, exhibited higher nitrogen and hydrogen hfsc's than PBN/O_2H, while those with electron-withdrawing substituents, 4-NC-PBN/O_2H and 4-MeNHCO-PBN/O_2H, exhibited lower a_N or $a_{\beta\text{-H}}$ values.

The increased a_N or $a_{\beta\text{-H}}$ value in the presence of electron-donating substituents could be due to higher contribution of the resonance form A (see Scheme 3). This increase in spin density on the nitrogen atom resulting in the increase of a_N and $a_{\beta\text{-H}}$ agrees well with the observation by Hinton and Janzen.[37] Correlation between Hammett σ constants and hfsc's of phenylnitrone adducts has been previously established[37,44] and shows that the electron-withdrawing para substituents on the phenyl ring decrease the a_N and $a_{\beta\text{-H}}$ while electron-donating groups increase them. Surprisingly, in the pyridine/H_2O_2 system, 4-HO_2C-PBN gave unusually high hfsc values (see Table 1) that do not correlate linearly with the σ_p. One explanation for the observed high a_N and $a_{\beta\text{-H}}$ for 4-HO_2C-PBN/O_2H could be due to the acid−base reaction between the pyridine and the carboxylic acid in which the major deprotonated form of the acid is present in pyridine solution. Comparison of the σ_p values shows that $-CO_2^-$ gave $\sigma_p = 0.00$ compared to $\sigma_p = 0.45$ for the $-CO_2H$ group, but the σ_p value for $-CO_2^-$ is not consistent with the general trend observed for the σ_p and hfsc correlation (Figure S1 in the Supporting Information). The calculated a_N and $a_{\beta\text{-H}}$ for the deprotonated 4-HO_2C-PBN/O_2H (Table 2) are highest compared to other spin adducts at various solvents, but it is more pronounced for $a_{\beta\text{-H}}$ with ~16.6 G compared to 0.7−12.0 G for the other adducts. For the sake of comparison, the other PBN derivatives were also added in the determination of the calculated hfsc values (Table S2 in the Supporting Information). As observed for the experimental hfsc's, a significant correlation between the σ_p values and the calculated a_N and $a_{\beta\text{-H}}$ values was found (Figure S3 in the Supporting Information), regardless of the solvent employed for the calculation.

C. Kinetics of Superoxide Radical Anion Addition. Recently, a new approach using a UV stopped-flow technique for the determination of the rate of $O_2^{\bullet-}$ trapping has been developed.[13] Phenol red was used as a probe to measure $O_2^{\bullet-}$ production at 575 nm, and the rate of formation of this new species at 575 nm (Figure 4) is directly proportional to the kinetics of $O_2^{\bullet-}$ decay. The kinetic values obtained using the stopped-flow technique have been shown to correlate well with the trends in rate constants obtained using the EPR technique.[13,45] We applied stopped-flow kinetics as an alternative method to further explore the polar effect of the substituent on the reactivity of $O_2^{\bullet-}$ with nitrones. Absorption intensities were normalized by subtracting the initial absorption at $t = 0$ s. Using the same experimental conditions used for the stopped-flow kinetics, the formation of the $O_2^{\bullet-}$ adducts were confirmed by EPR spectroscopy. The hfsc values are reported in Table 1, and the experimental and simulated spectra are shown in the Supporting Information (Figures S4 and S5).

As shown in Figure 4, addition of PBN to KO_2 solution results in a decrease of slope which becomes more apparent as the PBN concentration is increased. The initial rates of formation (i.e., the slope of the linear part of the curve as shown by the arrows) were determined and were plotted using eq 1, where V and v

SCHEME 2: Resonance Structures for PBN in the Presence of Electron-Donating (A) and Electron-Withdrawing Substituents (B)

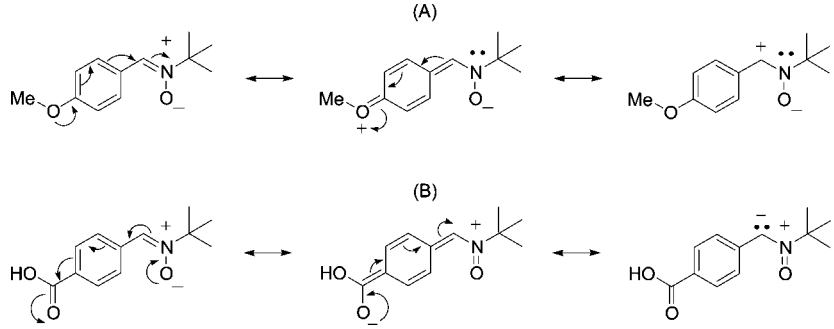

are the initial rates of $O_2^{\bullet-}$ addition to phenol red (PR) in the absence and presence of PBN derivatives, respectively.

$$\frac{V}{v} - 1 = \frac{k_{\text{X-PBN}}[\text{PBN}]}{k_{\text{PR}}[\text{PR}]} \quad (1)$$

The relative rate constants ($k_{\text{X-PBN}}/k_{\text{PR}}$) are reported in Table 3, and plots of (V/v) − 1 vs [X-PBN]/[PR] are reported in the Supporting Information (Figure S6). For the sake of comparison, we also obtained the rate of formation of DMPO in this study. Except for 4-HO_2C-PBN, all of the relative rates were significantly lower than 1, demonstrating that $O_2^{\bullet-}$ reacts faster with phenol red than with the PBN spin traps. The order of increasing rate of reactivity to $O_2^{\bullet-}$ is PBN < 4-NC-PBN ≈ 4-Me_2N-PBN ≈ 4-MeO-PBN < 4-MeNHCO-PBN < 4-$AcNHCH_2$-PBN < DMPO < 4-HO_2C-PBN. Using our previously[13] calculated rate constant for DMPO of $k_2 = 1.7\ M^{-1}\ s^{-1}$ gives k_2 values for PBN and its derivatives that range from 0.1 to 0.8 $M^{-1}\ s^{-1}$ (except for 4-HO_2C-PBN with $k_2 = 1.6 \times 10^3\ M^{-1}\ s^{-1}$) comparable to that observed for DEPMPO of 0.7 $M^{-1}\ s^{-1}$. The similar rate constants observed for 4-Me_2N-PBN, 4-NC-PBN, and 4-MeO-PBN clearly suggest that the polar substituent effect does not affect their reactivity with $O_2^{\bullet-}$ as these compounds exhibit scattered σ_p values: −0.83, 0.66, and −0.27, respectively (Figure 5a). No correlation with the rate constant of $O_2^{\bullet-}$ addition with nitronyl charge densities can be observed (Figure 5b).

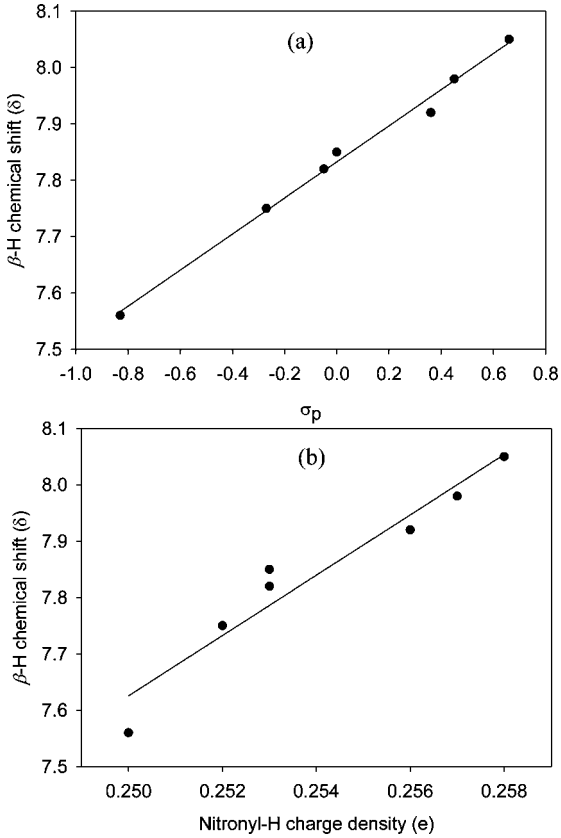

Figure 3. Correlation of β-H chemical shifts with (a) σ_p values ($R^2 = 0.992$) and (b) nitronyl-hydrogen charge densities ($R^2 = 0.930$). ^{1}H NMR chemical shifts were obtained using 300 mM nitrone in DMSO-d_6 with 2% $CHCl_3$ as internal reference.

TABLE 2: Calculated Hyperfine Splitting Constants of Nitroxyl Nitrogen (a_N) and β-Hydrogen ($a_{\beta\text{-H}}$) at the PCM/B3LYP/6-31+G(d,p)//B3LYP/6-31G(d) Level of Theory Using the Bulk Dielectric Effect of Water, DMSO, and Isoquinoline

	hfsc's of hydroperoxyl adducts (G)					
	in water		in DMSO		in isoquinoline	
nitrone	a_N	$a_{\beta\text{-H}}$	a_N	$a_{\beta-H}$	a_N	$a_{\beta-H}$
4-Me_2N-PBN (**1**)	14.8	12.0	14.8	12.0	14.7	11.9
4-MeO-PBN (**2**)	14.6	11.4	14.6	11.4	14.5	11.3
4-NC-PBN (**3**)	13.9	9.6	13.9	9.6	13.9	9.5
cis-4-HO_2C-PBN (**4**)	14.1	10.1	14.1	10.1	14.0	10.1
4-$^-O_2$C-PBN	14.7	16.7	14.8	16.6	14.8	16.6
4-MeNHCO-PBN (**5**)	12.3	5.0	12.2	4.9	12.0	4.9
4-$AcNHCH_2$-PBN (**9**)	14.0	0.7	14.0	0.7	13.9	0.7
PBN	14.3	10.6	14.3	10.6	14.3	10.5

SCHEME 3: Resonance Structures for 4-X-PBN/O_2H Adducts

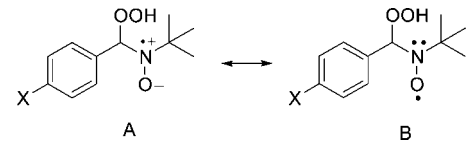

It has been shown that an electron-withdrawing substituent in PBN-type compounds increases the reactivity of the nitronyl group for nucleophilic addition reactions and nucleophilic radical addition.[13,46] On the contrary, nitrones bearing an electron-donating substituent have also been suggested to exhibit high reactivity to electrophilic radicals.[47,48] Unlike alicyclic nitrones,[13] the observed noncorrelation of the σ_p or C-charges with the rate of $O_2^{\bullet-}$ trapping observed for PBN derivatives could be due to the difference in the electrophilicity of the nitronyl-carbons in alicyclic nitrones and in aromatic PBN derivatives. ^{13}C NMR chemical shifts of 129.82 and 128.53 ppm in $CDCl_3$ and DMSO-d_6, respectively, were reported for the nitronyl-carbon of PBN by Chalier et al.,[49] while a chemical shift of 132.00 ppm was reported for DMPO in $CDCl_3$.[50] Therefore, the shielding on the

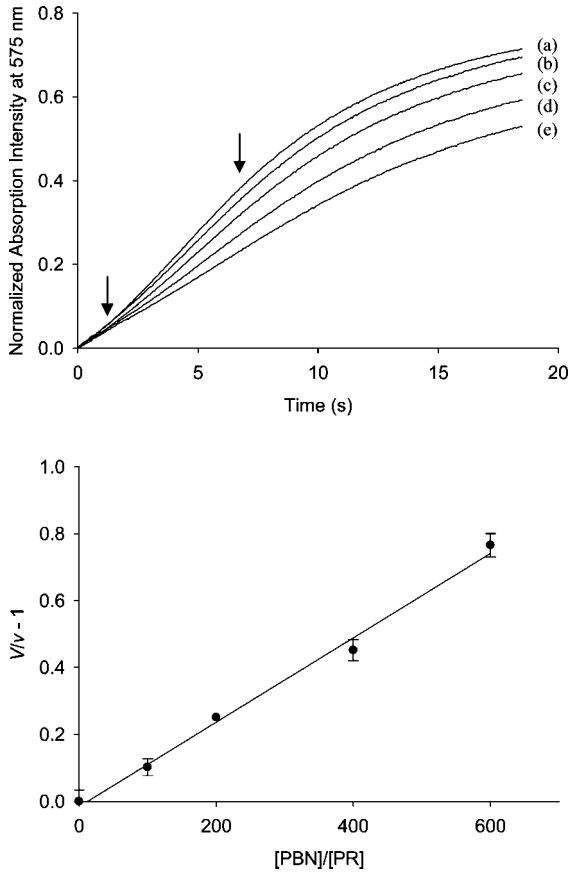

Figure 4. (top) Formation curve measured at 575 nm following mixing of KO_2 solution with varying PBN concentration containing 500 μM phenol red solution: (a) 0, (b) 50, (c) 100, (d) 200, and (e) 300 mM PBN. Arrows show the linear part of the curve. (bottom) Typical plot of $(V/v) - 1$ vs [PBN]/[PR] using the data shown above.

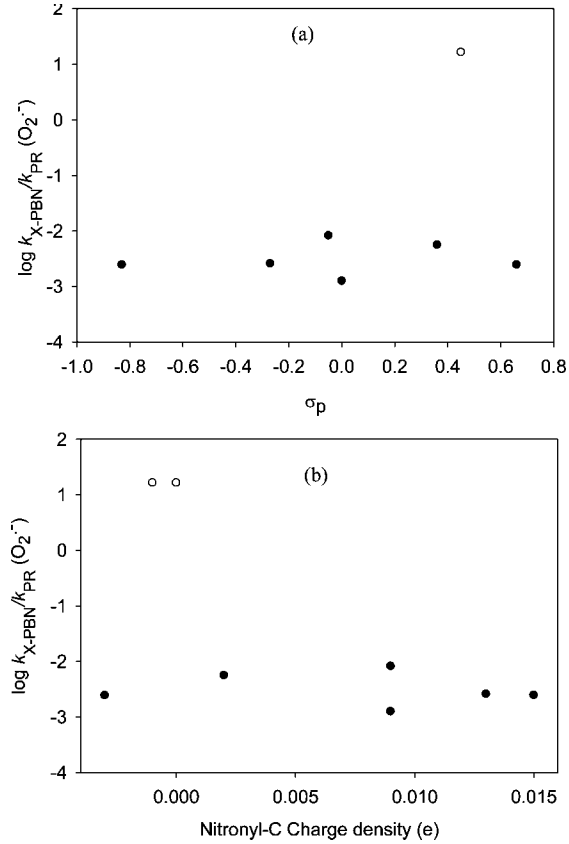

Figure 5. Plots of experimental relative rate constant of $O_2^{\bullet-}$ addition to X-PBN ($k_{X\text{-}PBN}/k_{PR}$) with (a) Hammett sigma values (σ_p) ($R^2 = 0.021$ excluding 4-HO_2C-PBN marked as ○) and (b) nitronyl-carbon charge densities ($R^2 = 0.022$ excluding *cis*- and *trans*-4-HO_2C-PBN marked as ○).

TABLE 3: Relative Rate Constants for $O_2^{\bullet-}$ and $HO_2^{\bullet}$ Adduct Formation in the DMF/KO_2 and Pyridine/H_2O_2 Systems

	DMF/KO_2[a]		pyridine/H_2O_2[b]	
compound	$k_{X\text{-}PBN}/k_{PR}$ (10^{-3})	R^2	$k_{X\text{-}PBN}/k_{DMPO}$ (10^{-3})	R^2
4-Me_2N-PBN (**1**)	2.5 ± 0.3[c]	0.910	14.3 ± 0.9[d]	0.935
			17.1 ± 2.3	0.767
4-MeO-PBN (**2**)	2.6 ± 0.1	0.974	7.2 ± 0.1	0.994
4-NC-PBN (**3**)	2.5 ± 0.2	0.941	19.7 ± 0.6	0.989
4-HO_2C-PBN (**4**)	$(1.6 \pm 0.1) \times 10^4$	0.933	38.8 ± 1.4[e]	0.981
4-MeNHCO-PBN (**5**)	5.6 ± 0.4	0.952	9.4 ± 0.1	0.997
4-$AcNHCH_2$-PBN (**9**)	8.3 ± 0.4	0.976	14.9 ± 0.4	0.984
PBN	1.3 ± 0.0	0.986	11.2 ± 0.3	0.988
DMPO	17.6 ± 0.5[f]	0.995	−	−

[a] Comparisons were performed with at least five different X-PBN concentrations ranging from 0 to 150 mM, with one to four runs per concentration. [b] Comparisons were performed with at least six different DMPO concentrations ranging from 0 to 10 mM, with one to five runs per concentration. [c] Only four concentrations. [d] DMPO concentration from 0 to 2 mM, six different concentrations. [e] DMPO concentration from 0 to 25 mM, six different concentrations and receiver gain 1×10^4. [f] Only three concentrations.

nitronyl-carbon is more apparent in the aromatic nitrone compared to the aliphatic one. Similarly, ^{13}C NMR of carbonyl carbon in aliphatic aldehyde gives a signal of ~201 ppm compared to the more upfield signal for benzaldehyde of ~191 ppm.[51] Similar to carbonyl compounds, nitrones are susceptible to nucleophilic addition reactions,[52] and therefore, the electronic nature of the nitronyl-carbon can affect its reactivity toward nucleophiles such as in the case of $O_2^{\bullet-}$. The trend in $O_2^{\bullet-}$ reactivity observed in alicyclic nitrones[52] may not follow that observed for PBN derivatives due to the difference in the electronic properties of their respective nitronyl-carbons. It can therefore be reasonably assumed that, due to the higher electron density observed on the nitronyl-carbon in PBN derivatives compared to the alicyclic nitrones, the nature of $O_2^{\bullet-}$ addition to PBN derivatives may be considered as a borderline case, i.e., partly electrophilic, which explains the observed noncorrelation between the rate constants and charge densities for the PBN derivatives.

The amide compounds, 4-MeNHCO-PBN and 4-$AcNHCH_2$-PBN, gave relative rate constants that are ~4.5 and ~6.5 times higher than that of PBN, respectively. The presence of electron-withdrawing substituents like amides increases the electron density on nitronyl-carbon as shown in Scheme 2 as well as the observed higher rate constant for $O_2^{\bullet-}$ reaction which further supports the partly electrophilic nature of $O_2^{\bullet-}$ addition to PBN derivatives. However, the reported polar effects of the two amide groups are quite different,[38] in which 4-$AcNHCH_2$− group has a σ constant of −0.05 exhibiting slightly electron-donating character while the 4-MeNHCO− group has a σ constant of +0.36. It is therefore conflicting to assume that the high reactivities of 4-MeNHCO-PBN and 4-$AcNHCH_2$-PBN are due to polar substituent effects. Also, one can assume that the amide group may play a role in the high rate of reaction observed for $O_2^{\bullet-}$. It has been observed that the amide compound 1-methyl-1-carbamoylcyclopentane (MCCP) which is devoid of nitrone moiety was able to form a strong amide-H···$O_2^{\bullet-}$ bond of

1.55−1.57 Å.[13] This strong H-bond interaction between the amide-H and $O_2^{\bullet-}$ causes perturbation in the electronic property of the $O_2^{\bullet-}$, hence facilitating the $O_2^{\bullet-}$ addition reaction as demonstrated using 5-carbamoyl-5-methylpyrroline *N*-oxide (AMPO) with $k \sim 130\ M^{-1}\ s^{-1}$.[13] It was also previously concluded that the contribution of the amide moiety to the rate of AMPO addition to $O_2^{\bullet-}$ is negligible since the rate constant of MCCP was slightly higher than that of DMPO, i.e., 2.0 and 1.7 $M^{-1}\ s^{-1}$, respectively. Although the position of the amide moiety in cyclic nitrones is different compared to PBN derivatives, H-bond interaction between the amide-H and $O_2^{\bullet-}$ along with the inductive polar effect could play a synergistic role in the enhanced reactivity of 4-MeNHCO-PBN and 4-$AcNHCH_2$-PBN to $O_2^{\bullet-}$ addition reaction[13] compared to other PBN derivatives.

Surprisingly, 4-HO_2C-PBN showed the highest reactivity with $k_{X\text{-}PBN}/k_{PR}$ of 16.5, which is ∼1000 and 13 000 times higher than that observed for DMPO and PBN, respectively. Typically, the stopped-flow kinetic experiments were performed using ∼100 mM concentration of PBN derivatives, but since no absorbance at 575 nm was observed after mixing 1 mM concentration of 4-HO_2C-PBN with KO_2 solution, kinetic studies using 4-HO_2C-PBN were only limited to the concentration range 0−125 μM. This extraordinarily high reactivity of $O_2^{\bullet-}$ to 4-HO_2C-PBN can be explained based on the ability of $O_2^{\bullet-}$ to act as a weak base. Superoxide radical anion has been shown to abstract protons from weak acids such as phenol.[53] Arylic carboxylic acids are stronger acids than phenols, e.g., the pK_a in water for benzoic acid and phenol is ∼4.2 and ∼9.9, respectively.[54] It can be assumed that 4-HO_2C-PBN can undergo reversible acid−base reaction with $O_2^{\bullet-}$ forming the more reactive hydroperoxyl radical ($HO_2^{\bullet}$);[55] i.e., $HO_2^{\bullet}$ is a stronger oxidizer than $O_2^{\bullet-}$ with $E^{\circ\prime} = 1.06$ and 0.94 V, respectively.[56] To further confirm the effect of carboxylic acid on $O_2^{\bullet-}$ reactivity, a similar kinetic study was carried out using benzoic acid and results showed a relative rate constant of 7.8 ± 0.6, which translates to about 6000 times more reactive than PBN alone. The kinetic results for 4-HO_2C-PBN and benzoic acid suggest that the carboxylic acid group plays a crucial role in the catalysis of $O_2^{\bullet-}$ addition to nitrones.

D. Kinetics of Hydroperoxyl Radical Trapping. The hydroperoxyl adducts were generated using H_2O_2 in pyridine.[57,58] The mechanism for hydroperoxyl adduct formation is not clear but is believed to occur via nucleophilic addition of HO_2^- to nitrone to yield the hydroxylamine and subsequent oxidation by O_2 to yield the aminoxyl adduct (see Scheme 4, reactions D and E). However, formation of 1,5- and 1,7-azulene quinone and enone derivatives from 4,6,8-trimethylazulene and guaiazulene using H_2O_2 in pyridine have been reported,[59] thus making a nucleophilic addition reaction of HO_2^- to the aromatic ring less probable. Also, the established pK_a[54] of the conjugate acid of pyridine is 5.2 while that of H_2O_2 is 11.6, and therefore an acid−base reaction between these two species is less likely to occur although HO_2^- had been previously generated but using stronger bases such as methoxide and hydroxide.[60] In the presence of a base, Roberts and co-workers[61] have suggested adduct formation arising from $HO^{\bullet}$ instead of $HO_2^{\bullet}$ with $a_N = 15.2 \pm 0.2$ G and $a_{H\text{-}\beta} = 2.8 \pm 0.2$ G using PBN as a spin trap in the pyridine/H_2O_2 system; however, this assignment was based on the expected spectral profile for PBN-OH versus PBN-O_2H in water. These reported hfsc's are significantly different from our reported hfsc's using the same radical generating system but in the absence of added base (Table 1). In this work, further proof of radical production was obtained using the nitronyl nitroxide, 2-(*p*-carboxyphenyl)-4,4,5,5,-tetramethylimidazoline-1-oxyl 3-oxide (carboxy-PTIO),[62] and shows quenching of the EPR signal in the presence of pyridine/H_2O_2 with significant line width broadening ($\Delta\Delta B_{pp} = 2.6$ G) suggesting a concomitant formation of O_2, perhaps from the $HO_2^{\bullet}$ dismutation. Moreover, the formation of the radical adduct using nitrone spin traps was not suppressed when H_2O_2 was added to the deoxygenated solution of a nitrone in pyridine, suggesting that the mechanism of adduct formation is not via a hydroxylamine intermediate.

SCHEME 4: Mechanisms for Hydroperoxyl Adduct Formation Using the Pyridine/H_2O_2 System[a]

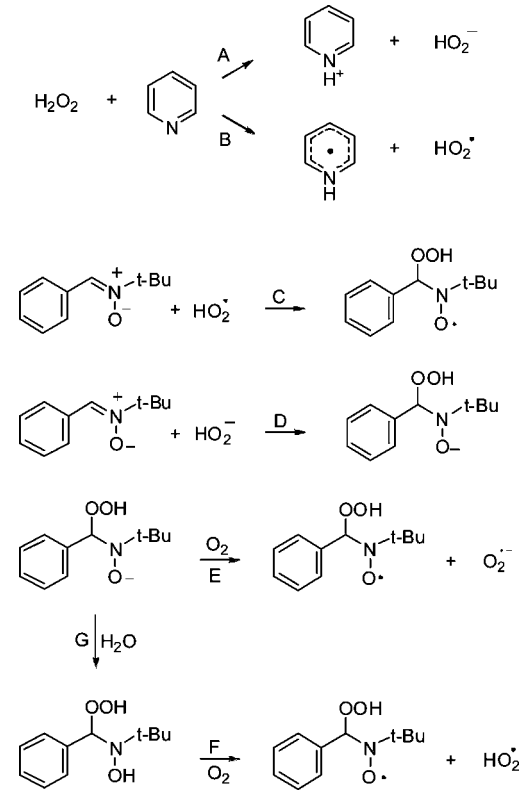

[a] The free energies of reaction ($\Delta G_{rxn,solvent,298\ K}$ in kcal/mol) in isoquinoline and water (in parentheses) are as follows: (A) 31.7 (22.6); (B) 45.6 (51.2); (C) −108.5 (−0.9); (D) −77.4 (29.0); (E) −25.4 (−22.3); (F) 16.9 (6.6); (G) −19.9 (−1.9); (A → D → E) −71.1 (29.3); (B → C) −63.0 (50.3).

To provide more insights into the mechanism of hydroperoxyl adduct formation from a PBN derivative in the pyridine/H_2O_2 system, the free energies of reactions were approximated using DFT method at the PCM/B3LYP/6-31+G**//B3LYP/6-31G* level. The dielectric effect of isoquinoline ($\varepsilon = 10.43$) was employed since pyridine ($\varepsilon = 13.26$)[54] is not implemented in the Gaussian 03 program.[34] Scheme 4 shows the free energies of reaction for the various pathways leading to the hydroperoxyl adduct formation using isoquinoline as solvent. Although the formation of $HO_2^{\bullet}$ is endoergic (reaction B), its formation is less favorable by ∼14 kcal/mol than the formation of HO_2^- (reaction A) with the radical addition pathway (i.e., B → C) being less preferred by 8 kcal/mol than the nucleophilic addition by HO_2^- (i.e., A → D → E). Based on these thermodynamic data, the preferred nucleophilic addition pathway does not agree with the experimental observations mentioned above. However, these calculated values do not represent other potential factors that can favor $HO_2^{\bullet}$ generation such as the effect of explicit solvent interaction with the reactants as well as the pertinent activation barriers.

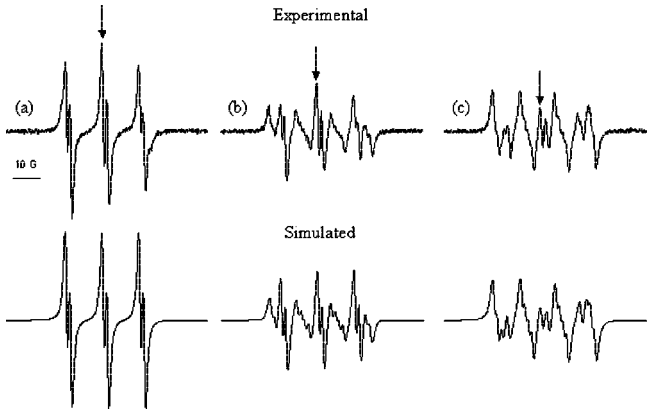

Figure 6. EPR spectra of 100 mM 4-AcNHCH$_2$-PBN with pyridine/H_2O_2 in the presence of (a) 0, (b) 2.5, and (c) 10 mM DMPO. All spectra were scaled on the same $x-y$ coordinate range. Arrows indicate the peak that is being monitored. Below each spectrum is its representative simulated spectrum.

The relative rate constants for the hydroperoxyl adduct formation from 4-Me$_2$N-PBN, 4-NC-PBN, 4-MeO-PBN, 4-HO$_2$C-PBN, 4-MeNHCO-PBN, 4-AcNHCH$_2$-PBN, and PBN were determined by EPR using competition kinetics with DMPO (Table 3). Figure 6 shows representative spectra of 4-AcNHCH$_2$-PBN/O_2H in the presence of DMPO/O_2H at various DMPO concentrations. There was no serious overlap between the two adducts, and no significant shift in the maximum peak intensity was observed when the concentrations of DMPO become higher.

Peak height intensities of the second peak of the PBN derivative were monitored 42 s after addition of 30% H_2O_2 to the nitrone solution in pyridine. Peak growth is linear during the first minute of measurement and then begins to deviate from linearity thereafter. Addition of DMPO to the solutions of PBN derivative results in a lower rate of signal formation which negatively correlates with the concentration of DMPO. The decrease in peak intensity of the second peak of the PBN was monitored, and the initial rates of formation were determined for 1 min. The peak intensities were normalized by subtracting the value of the peak intensity at time 0 s and were fitted to a linear equation. The data were then plotted using eq 2, where V and v are the initial rates of HO_2 adduct formation (i.e., the slope of the linear-fitted equation) in the absence and presence of DMPO, respectively.

$$\frac{V}{v} - 1 = \frac{k_{\text{DMPO}}[\text{DMPO}]}{k_{\text{X-PBN}}[\text{PBN}]} \qquad (2)$$

Plots of $(V/v) - 1$ vs [DMPO]/[X-PBN] are shown in Figure 7 and the Supporting Information (Figure S7).

The inverse of the relative rate constant $K = (k_{\text{X-PBN}}/k_{\text{DMPO}})$ (Table 3) was used for convenience. In subsequent discussion, the relative rate constant will be referred to as K; thus, the higher the K ratio, the faster the spin trapping by X-PBN. All the relative rate constants observed were in the range $(7.15-38.78) \times 10^{-3}$, demonstrating that the trapping rate of DMPO is at least 2 orders of magnitude higher compared to the PBN derivatives. However, there are significant differences in the rates of hydroperoxyl adduct formation using PBN derivatives. 4-Me$_2$N-PBN/O_2H showed a very weak EPR signal even in the absence of DMPO. For example, after integration of the simulated EPR spectra of 4-Me$_2$N-PBN/O_2H and DMPO/O_2H after ~3 min using 100 mM 4-Me$_2$N-PBN and 2 mM DMPO, respectively, revealed that 66% of the adducts formed is due to DMPO, suggesting that 4-Me$_2$N-PBN is a less efficient trap

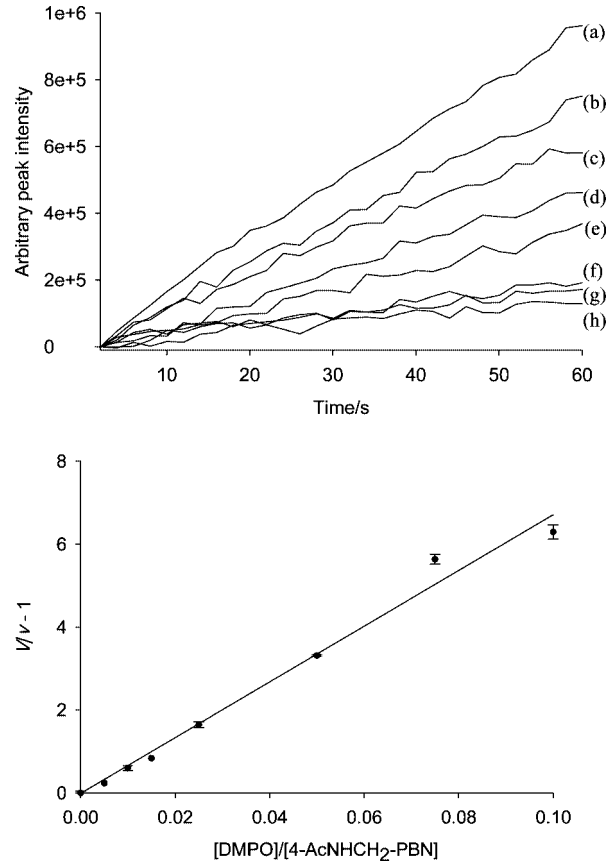

Figure 7. (top) Formation of the middle EPR signal during competitive trapping of 100 mM nitrone 4-AcNHCH$_2$-PBN with (a) 0, (b) 0.5, (c) 1, (d) 1.5, (e) 2.5, (f) 5, (g) 7.5, and (h) 10 mM DMPO. (bottom) Typical plot of $(V/v) - 1$ vs [DMPO]/[4-AcNHCH$_2$-PBN] using the data shown above.

compared to DMPO. Due to the weak signal intensity of 4-Me$_2$N-PBN/O_2H, a high standard error was observed even when the kinetic measurement was performed using a very low concentration of DMPO (molar ratio of 200:1). To rationalize the low signal intensity observed for 4-Me$_2$N-PBN, the effect of the amino group on the electronic properties of 4-Me$_2$N-PBN was further investigated. The σ_p values for $-NH_2$ and $-NH_3^+$ are -0.66 and 0.60, respectively, so we expect that 4-Me$_2$NH$^+$-PBN will exhibit a higher spin trapping rate, but this is inconsistent with our experimentally observed rate constants. Another plausible explanation for the low adduct yield for 4-Me$_2$N-PBN could be its stability. While the pK_a for *N*,*N*-dimethylaminobenzene is unknown, the reported pK_a for tertiary amines is on the order of ~10−12.[63] Therefore, based on the known pK_a of 5.23[54] for pyridine, it can be assumed that the high basic property of the dimethylamino moiety may have a significant effect on the stability of the hydroperoxyl adduct. Base-catalyzed decomposition of the superoxide adduct of DMPO,[64] DEPMPO,[65] and BocMPO[66] in mildly basic pH has been reported. Although the exact mechanism for this decomposition is unclear, Kharasch et al.[67] and Rosen et al.[2] proposed that base catalyzed decomposition of hydroperoxide leads to the formation of alcohol and molecular oxygen.

A plot of log K versus σ_p values is shown in Figure 8a, and a general trend can be observed where the rate constant increases with increasing σ_p value. A satisfactory correlation can be observed in which lower reactivity was observed on nitrones bearing a more positive nitronyl-carbon (Figure 8b). These observations are similar to that previously observed by Schmid

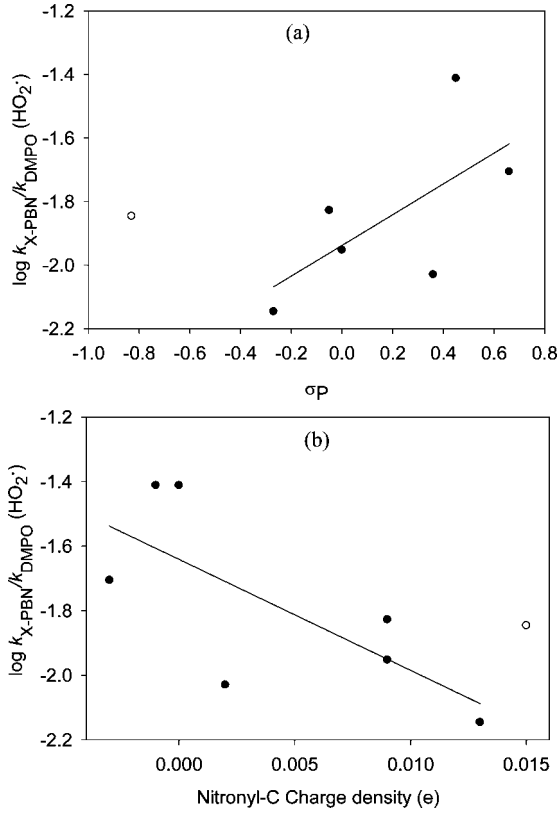

Figure 8. Correlation of experimental relative rate constant of hydroperoxyl adduct formation from X-PBN with (a) Hammett sigma values (σ_p) ($R^2 = 0.42$ excluding the outlier 4-Me_2N-PBN marked as ○) and (b) nitronyl-carbon charge densities ($R^2 = 0.53$ excluding the outlier 4-Me_2N-PBN marked as ○).

TABLE 4: Polar Effects on Relative Rate Constant ($k_{X\text{-}PBN}/k_{PBN}$) of Spin Trapping Reactions

radical	ρ	R^2	ref
cyclo$C_6H_{11}CO_2^{\bullet}$	−1.02	0.955	Abe et al.[48]
	−0.51[a]	0.997[a]	
$C_6H_5CO_2^{\bullet}$	−0.63	0.908	Janzen et al.[69]
tert-$BuO^{\bullet}$	−0.30	0.979	Abe et al.[48]
	0.3	0.678	Janzen et al.[73]
	0.27[b]	0.998[b]	
$HO^{\bullet}$	0.35	0.654	Sueishi et al.[70]
n-alkyl$^{\bullet}$	0.29	0.808	Schmid and Ingold[68]
	0.21[c]	0.988[c]	
$Et^{\bullet}$	0.76	0.998	Sueishi et al.[46]
$Me^{\bullet}$	0.76	0.938	Sueishi et al.[46]
$HO_2^{\bullet}$	0.48	0.425	this work
	0.45[d]	0.972[d]	

[a] Determined from the linear part. [b] Determined with positive σ_p values. [c] Determined with negative σ_p values. [d] Determined with compounds **2**, **3**, and PBN.

and Ingold[68] on the addition of *n*-alkyl radicals to nitrones, but the polar effect is much larger in our case with $\rho = 0.48$ compared to their reported $\rho = 0.21$ determined with negative σ_p values or $\rho = 0.29$ using a whole series (Table 4). Interestingly, Janzen, et al.[69] found an opposite polar effect with benzoyloxy radicals ($\rho = -0.47$ determined with the positive σ_p values or $\rho = -0.63$ using a whole series), but concluded that one may expect a less negative slope (maybe positive) for a nucleophilic radical. Recently, Sueshi et al.[46] also reported the faster addition of methyl and ethyl alkyl radicals on PBN bearing an electron-withdrawing group with $\rho = 0.76$ supporting the notion that alkyl radical reactivity is nucleophilic in nature while benzoyloxy radical addition to nitrone is electrophilic. Based on an electron-transfer mechanism and molecular orbital calculation for the radical reaction with nitrones, Hirota et al. found that the frontier orbital energy difference between the LUMO of the free radicals with electronegative centers such as *tert*-butoxyl and carboxyl radicals and the HOMO of the spin traps becomes smaller as the substituent on the spin trap becomes more electron-donating, therefore increasing the rate of radical addition to nitrones.[48] Thus, they reported reaction constants of −0.51 and −0.30 (determined from the linear part of the Hammett plot) for the electronegative carboxyl and *tert*-butoxy radical trapping, respectively. On the contrary, the spin trapping of carbon-centered radicals results in the decrease in the difference in frontier orbital energies as the substituent becomes electron-withdrawing and the rate of trapping by PBN is increased as the substituent becomes more electron-withdrawing, as reported elsewhere.[46,47,68]

Figure 8 suggests that hydroperoxyl adduct formation is favored when the nitronyl-carbon charge density is lower. Therefore, $HO_2^{\bullet}$ addition to nitrones appears to be more favored in the presence of electron-withdrawing substituents. Based on the resonance structures shown in Scheme 2, the presence of an electron-withdrawing group increases the negative character of the nitronyl-carbon, which is further supported by the calculated charge densities on the nitronyl-carbon (Table 1). This suggests that $HO_2^{\bullet}$ addition to nitrones is electrophilic in nature. Finally, theoretical calculations using DFT method also suggests the possibility that the hydroperoxyl adduct formation may involve radical addition of $HO_2^{\bullet}$ rather than nucleophilic addition of HO_2^- (Scheme 4).

Based on the observed correlation between the nitronyl-carbon charge densities with the σ_p values of the substituents (Figure 2a), the conclusions reported in the literature regarding the nature of radical addition to nitrone are inconsistent (Table 4). For example, while it has been suggested that the positive ρ values are due to the nucleophilic character of the radicals as observed for alkyl,[46,68] hydroxyl, and phenyl radicals,[70] we found in the present work that a positive ρ value may be due to the electrophilicity of $HO_2^{\bullet}$. Thus, the observed positive slope for $HO^{\bullet}$ trapping by PBN derivatives, and the conclusion that $HO^{\bullet}$ addition to nitrones is nucleophilic in nature,[70] is contrary to the recent report by De Vleeschouwer et al.[32] which demonstrates the electrophilic character of $HO^{\bullet}$ using natural population analysis. Moreover, this latter group also concluded a moderate nucleophilic nature for $^{\bullet}CH_3$ that is in agreement with the conclusion of Sueishi et al.[46] but still remains controversial based on the nitronyl-carbon charge densities. It therefore has become apparent that the sign of the ρ value is generally dependent on the nature of radical addition and not on the intrinsic characteristic of the radical itself.

The influence of adduct decay on the kinetics of spin trapping was also investigated. After 1 h of HO_2 adduct formation, no significant decrease in the EPR signal intensity was observed for 4-Me_2N-PBN, 4-MeO-PBN, 4-MeNHCO-PBN, and 4-HO_2C-PBN hydroperoxyl adducts, while significant HO_2 adduct decay can be observed for 4-$AcNHCH_2$-PBN and PBN after 30 min. Therefore, it can be concluded that the adduct decay does not interfere with the initial rate of spin trapping and is consistent with the work of Taniguchi and Madden, who demonstrated that the rates of spin trapping are much higher than their respective decay rates.[71] The longer stability of hydroperoxyl adducts of cyclic nitrones in organic solvent than in aqueous milieu has also been demonstrated.[57,65] Also, a long lifetime

TABLE 5: Free Energies ($\Delta G_{rxn,298\ K}$) of $O_2^{\bullet-}$ and $HO_2^{\bullet}$ Addition with Para-Substituted PBN Derivatives at the PCM/B3LYP/6-31+G(d,p)//B3LYP/6-31G(d) Level of Theory in DMSO and Isoquinoline, Respectively[a]

$O_2^{\bullet-}$ addition			$HO_2^{\bullet}$ addition		
nitrone	$\Delta G_{rxn,298\ K}$ in DMSO (water)	nitronyl-carbon charge density (e) in DMSO	nitrone	$\Delta G_{rxn,298\ K}$ in isoquinoline (water)	nitronyl-carbon charge density (e) in isoquinoline
4-HO_2C-PBN (**4**)	17.6 (16.9)	0.000	4-NH_2CO-PBN	−108.9 (0.2)	−0.001
4-NO_2-PBN	18.9 (18.2)	−0.004	4-HO_2C-PBN (**4**)	−108.7 (−0.0)	−0.003
PBN	18.9 (18.3)	0.010	4-HO-PBN	−108.6 (−0.4)	0.012
4-SO_3-PBN	19.9 (19.0)	0.013	PBN	−108.5 (−0.9)	0.007
4-MeO_2PO-PBN	20.0 (19.7)	−0.011	4-NC-PBN (**3**)	−108.3 (0.4)	−0.005
4-NC-PBN (**3**)	20.2 (19.7)	−0.002	4-MeO-PBN (**2**)	−108.2 (0.1)	0.011
4-$AcNHCH_2$-PBN (**9**)	20.3 (19.1)	0.009	4-NH_2-PBN	−108.0 (0.3)	0.013
4-MeO-PBN (**2**)	20.4 (19.5)	0.014	4-NO_2-PBN	−108.0 (0.6)	−0.007
4-HO-PBN	20.5 (19.7)	0.015	4-MeO_2PO-PBN	−108.0 (−0.3)	−0.012
4-NH_2CO-PBN	21.2 (20.6)	0.002	4-Me_2N-PBN (**1**)	−108.0 (0.2)	0.013
4-MeNHCO-PBN (**5**)	21.5 (21.0)	0.003	4-$AcNHCH_2$-PBN (**9**)	−96.2 (0.3)	0.006
4-NH_2-PBN	21.6 (21.0)	0.016	4-MeNHCO-PBN (**5**)	−91.8 (1.7)	0.000
4-Me_2N-PBN (**1**)	22.2 (21.4)	0.016	4-SO_3-PBN	−91.4 (3.1)	0.012
4-AcNH-PBN	25.5 (24.8)	0.011	4-AcNH-PBN	−91.1 (1.1)	0.008

[a] Values in parentheses are free energies of reaction in water.

for a hydroperoxyl adduct of a phosphorylated PBN derivative (4-HOPPN) in pyridine has been reported.[72]

E. Thermodynamics of Adduct Formation. Table 5 shows the free energies ($\Delta G_{rxn,298\ K}$) of $O_2^{\bullet-}$ and $HO_2^{\bullet}$ addition to para-substituted PBN derivatives at the PCM/B3LYP/6-31+G(d,p)//B3LYP/6-31G(d) level of theory in DMSO and isoquinoline, respectively. The solvents, DMSO and isoquinoline, were chosen to give better estimates of the thermodynamics of addition in DMF and pyridine, where the kinetic experiments for $O_2^{\bullet-}$ and $HO_2^{\bullet}$ were performed, respectively. In general, the free energies of reaction are <1 kcal/mol less favorable in water compared to in DMSO for $O_2^{\bullet-}$, while the energy difference in $HO_2^{\bullet}$ reactivity in water versus isoquinoline was significant with an energy difference of ∼90−110 kcal/mol, indicating the difference in the polarity of $O_2^{\bullet-}$ and $HO_2^{\bullet}$. Moreover, results show that no correlation can be observed for $\Delta G_{rxn,298\ K}$ and nitronyl-carbon charge densities in both $O_2^{\bullet-}$ and $HO_2^{\bullet}$ addition reactions. This further validates our experimental data that show the non-nucleophilic characters of $O_2^{\bullet-}$ and $HO_2^{\bullet}$ addition to para-substituted PBN derivatives. It is important to note that, in general, amide substitution gives the least reactivity to $O_2^{\bullet-}$ and $HO_2^{\bullet}$ while carboxylic acid substitution gives the most favorability. This trend in the thermodynamics of $O_2^{\bullet-}$ addition to PBN analogues is contrary to that observed for cyclic nitrones in which the amide substitution at the C-5 position gave the most favorable reaction.[13]

IV. Conclusion

Two novel para amido-substituted PBNs were synthesized as well as dimethyl amino, methoxy, carboxylic acid, and cyano para-substituted PBN compounds. The spin trapping rates of $O_2^{\bullet-}$ and $HO_2^{\bullet}$ radicals to the PBN derivatives were experimentally determined using UV−vis stopped-flow kinetic method and EPR-based competition kinetics, while computational studies using DFT were used to predict the nitronyl atom charge densities and the free energies of $O_2^{\bullet-}$ and $HO_2^{\bullet}$ addition to nitrones. The experimental kinetic data showed that the addition of $O_2^{\bullet-}$ is not affected by the polar substituent effect while the $HO_2^{\bullet}$ trapping follows Hammett's equation. Theoretical calculations were also employed to assess the thermodynamics of $O_2^{\bullet-}$ and $HO_2^{\bullet}$ addition to PBN derivatives, and results show that these reactions do not correlate with the calculated charge densities on the nitronyl-carbon. This combination of experimental and theoretical studies provided new insight into the reactivity of $O_2^{\bullet-}$ and $HO_2^{\bullet}$ with PBN derivatives; i.e., while the nature of $HO_2^{\bullet}$ addition to the nitronyl group was found to be predominantly electrophilic, $O_2^{\bullet-}$ was found to be only weakly electrophilic. These findings on the reactivity of $O_2^{\bullet-}$ and $HO_2^{\bullet}$ toward PBN derivatives can provide leads toward the design of novel PBN-type compounds with improved spin trapping properties for analytical and therapeutic applications.

Acknowledgment. This publication was made possible by Grant HL 81248 from the NIH National Heart, Lung, and Blood Institute. This work was supported in part by an allocation of computing time from the Ohio Supercomputer Center. We thank Prof. Valery Khramtsov and Dr. Andrey Bobko for EPR studies using carboxy-PTIO.

Supporting Information Available: General procedure for the synthesis of compounds **1**−**4**; correlations of the σ_p values with the N- and H-hyperfine splitting constants in pyridine/H_2O_2 and DMF/KO_2 systems; correlations of the σ_p values with the calculated N- and H-hyperfine splitting constants of hydroperoxyl adducts at the PCM/B3LYP/6-31+G(d,p)//B3LYP/6-31G(d) level of theory using the bulk dielectric effect of water; experimental and simulated EPR spectra of compounds **1**−**5** and **9** spin adducts in DMF/KO_2 system; plots of $V/v - 1$ vs [X-PBN]/[Phenol Red] and $V/v - 1$ vs [DMPO]/[X-PBN]; calculated hyperfine splitting constants of hydroperoxyl adducts at the PCM/B3LYP/6-31+G(d,p)//B3LYP/6-31G(d) level of theory using the bulk dielectric effect of water, DMSO, and isoquinoline. This material is available free of charge via the Internet at http://pubs.acs.org.

References and Notes

(1) Villamena, F. A.; Zweier, J. L. *Antioxid. Redox Signaling* **2004**, *6*, 619.

(2) Rosen, G. M.; Britigan, B. E.; Halpern, H. J.; Pou, S. *Free Radicals: Biology and Detection By Spin Trapping*; Oxford Univeristy Press: New York, 1999.

(3) Roubaud, V.; Lauricella, R.; Tuccio, B.; Bouteiller, J.-C.; Tordo, P. *Res. Chem. Intermed.* **1996**, *22*, 405.

(4) Frejaville, C.; Karoui, H.; Tuccio, B.; Moigne, F. L.; Culcasi, M.; Pietri, S.; Lauricella, R.; Tordo, P. *J. Med. Chem.* **1995**, *38*, 258.

(5) Zeghdaoui, A.; Tuccio, B.; Finet, J.-P.; Cerri, V.; Tordo, P. *J. Chem. Soc., Perkin Trans. 2* **1995**, 2087.
(6) Murphy, M. L. P.; Echtay, K. S.; Blaikie, F. H.; Asin-Cayuela, J.; Cocheme, H. M.; Green, K.; Buckingham, J. A.; Taylor, E. R.; Hurrell, F.; Hughes, G.; Miwa, S.; Cooper, C. E.; Svistunenko, D. A.; Smith, R. A. J.; Brand, M. D. *J. Biol. Chem.* **2003**, *278*, 48534.
(7) Hardy, M.; Ouari, O.; Charles, L.; Finet, J.-P.; Iacazio, G.; Monnier, V.; Rockenbauer, A.; Tordo, P. *J. Org. Chem.* **2005**, *70*, 10426.
(8) Poeggeler, B.; Durand, G.; Polidori, A.; Pappolla, M. A.; Vega-Naredo, I.; Coto-Montes, A.; Boeker, J.; Hardeland, R.; Pucci, B. *J. Neurochem.* **2005**, *95*, 962.
(9) Durand, G.; Poeggeler, B.; Boeker, J.; Raynal, S.; Polidori, A.; Pappolla, M. A.; Hardeland, R.; Pucci, B. *J. Med. Chem.* **2007**, *50*, 3976.
(10) Halliwell, B.; Gutteridge, J. M. C. *Free Radicals in Biology and Medicine*; Oxford University Press: Oxford, U.K., 2007.
(11) Delattre, J.; Beaudeux, J.-L.; Bonnefont-Rousselot, D. *Radicaux Libres et Stress Oxydant*; Lavoisier: Paris, 2005.
(12) Floyd, R. A.; Hensley, K. *Ann. N. Y. Acad. Sci.* **2000**, *899*, 222. Packer, L.; Cadenas, E. *Handbook of Synthetic Antioxidants*; Marcel Dekker, Inc.: New York, 1997.
(13) Villamena, F. A.; Xia, S.; Merle, J. K.; Lauricella, R.; Tuccio, B.; Hadad, C. M.; Zweier, J. L. *J. Am. Chem. Soc.* **2007**, *129*, 8177.
(14) Gotoh, N.; Niki, E. *Chem. Lett.* **1990**, 1475.
(15) Novelli, G. P.; Angiolini, P.; Tani, R.; Consales, G.; Bordi, L. *Free Radical Res. Commun.* **1986**, *1*, 321.
(16) Cao, X.; Phillis, J. W. *Brain Res.* **1994**, *644*, 267.
(17) Mori, H.; Arai, T.; Ishii, H.; Adachi, T.; Endo, N.; Makino, K.; Mori, K. *Neurosci. Lett.* **1998**, *241*, 99.
(18) Jotti, A.; Paracchini, L.; Perletti, G.; Piccinini, F. *Pharmacol. Res.* **1992**, *26*, 143.
(19) Parman, T.; Wiley, M. J.; Wells, P. G. *Nat. Med.* **1999**, *5*, 582.
(20) Floyd, R. A.; Hensley, K.; Forster, M. J.; Kelleher-Andersson, J. A.; Wood, P. L. *Mech. Ageing Dev.* **2002**, *123*, 1021.
(21) Floyd, R. A. *Aging Cell* **2006**, *5*, 51.
(22) Green, A. R. *Crit. Rev. Neurobiol.* **2004**, *16*, 91.
(23) Maurelli, E.; Culcasi, M.; Delmas-Beauvieux, M.-C.; Miollan, M.; Gallis, J.-L.; Tron, T.; Pietri, S. *Free Radical Biol. Med.* **1999**, *27*, 34. Pietri, S.; Liebgott, T.; Frejaville, C.; Tordo, P.; Culcasi, M. *Eur. J. Biochem.* **1998**, *254*, 256. Tosaki, A.; Blasig, I. E.; Pali, T.; Ebert, B. *Free Radical Biol. Med.* **1990**, *8*, 363.
(24) Hardy, M.; Rockenbauer, A.; Vasquez-Vivar, J.; Felix, C.; Lopez, M.; Srinivasan, S.; Avadhani, N.; Tordo, P.; Kalyanaraman, B. *Chem. Res. Toxicol.* **2007**, *20*, 1053.
(25) Morandat, S.; Durand, G.; Polidori, A.; Desigaux, L.; Bortolato, M.; Roux, B.; Pucci, B. *Langmuir* **2003**, *19*, 9699.
(26) Durand, G.; Polidori, A.; Ouari, O.; Tordo, P.; Geromel, V.; Rustin, P.; Pucci, B. *J. Med. Chem.* **2003**, *46*, 5230.
(27) Ortial, S.; Durand, G.; Poeggeler, B.; Polidori, A.; Pappolla, M. A.; Boeker, J.; Hardeland, R.; Pucci, B. *J. Med. Chem.* **2006**, *49*, 2812.
(28) Ouari, O.; Chalier, F.; Bonaly, R.; Pucci, B.; Tordo, P. *J. Chem. Soc., Perkin Trans. 2* **1998**, 2299.
(29) Duling, D. R. *J. Magn. Reson., Ser. B* **1994**, *104*, 105.
(30) Labanowski, J. W.; Andzelm, J. *Density Functional Methods in Chemistry*; Springer: New York, 1991. Parr, R. G.; Yang, W. *Density Functional Theory in Atoms and Molecules*; Oxford University Press: New York, 1989.
(31) Becke, A. D. *Phys. Rev.* **1988**, *38*, 3098. Becke, A. D. *J. Chem. Phys.* **1993**, *98*, 1372. Hehre, W. J.; Radom, L.; Schleyer, P. V.; Pople, J. A. *Ab Initio Molecular Orbital Theory*; John Wiley & Sons: New York, 1986.
(32) DeVleeschouwer, F.; VanSpeybroeck, V.; Waroquier, M.; Geerlings, P.; DeProft, F. *Org. Lett.* **2007**, *9*, 2721.
(33) Barone, V.; Cossi, M.; Tomasi, J. *J. Chem. Phys.* **1997**, *107*, 3210. Barone, V.; Cossi, M.; Tomasi, J. *J. Comput. Chem.* **1998**, *19*, 404. Tomasi, J.; Mennucci, B.; Cossi, M.; Barone, V.; Cammi, R.; Tomasi, J. *Chem. Phys. Lett.* **1996**, *255*, 327. Cammi, R. *Chem. Rev.* **2005**, *105*, 2999. Tomasi, J.; Persico, M. *Chem. Rev.* **1994**, *94*, 2027.
(34) Frisch, M. J. et al. *Gaussian 03*, revision B.04; Gaussian, Inc.: Pittsburgh, PA, 2003.
(35) Reed, A. E.; Curtiss, L. A.; Weinhold, F. A. *Chem. Rev.* **1988**, *88*, 899.
(36) Scott, A. P.; Radom, L. *J. Phys. Chem.* **1996**, *100*, 16502.
(37) Hinton, R. D.; Janzen, E. G. *J. Org. Chem.* **1992**, *57*, 2646.
(38) Hansch, C.; Leo, A.; Taft, R. W. *Chem. Rev.* **1991**, *91*, 165.
(39) SDBSWeb; http://riodb01.ibase.aist.go.jp/sdbs/. National Institute of Advanced Industrial Science and Technology, May 1, 2008.
(40) Burgett, R. A.; Bao, X.; Villamena, F. A. *J. Phys. Chem. A* **2008**, *112*, 2447.
(41) Janzen, E. G. Stereochemistry of Nitroxides. In *Topics in Streochemistry*; Allinger, L. L., Eliel, E. L., Eds.; Wiley-Interscience: New York, 1971; Vol. 6; p 186.
(42) Villamena, F. A.; Merle, J. K.; Hadad, C. M.; Zweier, J. L. *J. Phys. Chem. A* **2005**, *109*, 6089.
(43) Han, Y.; Tuccio, B.; Lauricella, R.; Rockenbauer, A.; Zweier, J. L.; Villamena, F. A. *J. Org. Chem.* **2008**, *73*, 2533.
(44) Janzen, E. G. *Acc. Chem. Res.* **1969**, *2*, 279.
(45) Allouch, A.; Roubaud, V.; Lauricella, R.; Bouteiller, J.-C.; Tuccio, B. *Org. Biomol. Chem.* **2005**, *3*, 2458.
(46) Sueishi, Y.; Yoshioka, D.; Yoshioka, C.; Yamamoto, S.; Kotake, Y. *Org. Biomol. Chem.* **2006**, *4*, 896.
(47) Murofushi, K.; Abe, K.; Hirota, M. *J. Chem. Soc., Perkin Trans. 2* **1987**, 1829.
(48) Abe, Y.; Seno, S.; Sakakibara, K.; Hirota, M. *J. Chem. Soc., Perkin Trans. 2* **1991**, 897.
(49) Chalier, F.; Ouari, O.; Tordo, P. *Org. Biomol. Chem.* **2004**, *2*, 927.
(50) Black, D. S. C.; Strauch, R. J. *Magn. Reson. Chem.* **1991**, *29*, 1114. Janzen, E. G.; Haire, D. L. *Adv. Free Radical Chem.* **1990**, *1*, 253.
(51) *The Chemist's Companion: A Handbook of Practical Data, Techniques, and References*; Gordon, A. J., Ford, R. A., Eds.;Wiley-Interscience: New York, 1972.
(52) Breuer, E.; Aurich, H. G.; Nielsen, A. *Nitrones, Nitronates and Nitroxides*; John Wiley and Sons: New York, 1989. Torssell, K. B. G. *Nitrile Oxides, Nitrones, and Nitronates in Organic Synthesis: Novel Strategies in Synthesis*; VCH: New York, 1988.
(53) Andrieux, C. P.; Hapiot, P.; Saveant, J. M. *J. Am. Chem. Soc.* **1987**, *109*, 3768.
(54) Lide, D. R. *CRC Handbook of Chemistry and Physics*; CRC Press: Boca Raton, FL, 2002.
(55) Villamena, F. A.; Merle, J. K.; Hadad, C. M.; Zweier, J. L. *J. Phys. Chem. A* **2007**, *111*, 9995.
(56) Buettner, G. R. *Arch. Biochem. Biophys.* **1993**, *300*, 535.
(57) Reszka, K.; Bilski, P.; Chignell, C. F. *Free Radical Res. Commun.* **1992**, *17*, 377.
(58) Tuccio, B.; Zeghdaoui, A.; Finet, J.-P.; Cerri, V.; Tordo, P. *Res. Chem. Intermed.* **1996**, *22*, 393.
(59) Matsubara, Y.; Morita, M.; Takekuma, S.; Nakano, T.; Yamamoto, H.; Nozoe, T. *Bull. Chem. Soc. Jpn.* **1991**, *64*, 3497.
(60) Buncel, E.; Wilson, H.; Chuaqui, C. *J. Am. Chem. Soc.* **1982**, *104*, 4896. Jones, D. D.; Johnson, D. C. *J. Org. Chem.* **1967**, *32*, 1402.
(61) Roberts, J. L., Jr.; Morrison, M. M.; Sawyer, D. T. *J. Am. Chem. Soc.* **1978**, *100*, 329.
(62) Goldstein, S.; Russo, A.; Samuni, A. *J. Biol. Chem.* **2003**, *278*, 50949.
(63) Frenna, V.; Vivona, N.; Consiglio, G.; Spinelli, D. *J.Chem. Soc., Perkin Trans. 2* **1985**, 1865. Hall, H. K. *J. Am. Chem. Soc.* **1957**, *79*, 5444. Hall, H. K. *J. Am. Chem. Soc.* **1957**, *79*, 5441.
(64) Buettner, G. R.; Oberley, L. W. *Biochim. Biophys. Acta* **1978**, *808*, 235.
(65) Tuccio, B.; Lauricella, R.; Frejaville, C.; Bouteiller, J.-C.; Tordo, P. *J. Chem. Soc., Perkin Trans. 2* **1995**, 295.
(66) Villamena, F. A.; Zweier, J. L. *J. Chem. Soc., Perkin Trans. 2* **2002**, 1340.
(67) Kharasch, M. S.; Fono, A.; Nudenberg, W.; Bruno, B. *J. Org. Chem.* **1952**, *17*, 207.
(68) Schmid, P.; Ingold, K. U. *J. Am. Chem. Soc.* **1978**, *100*, 2493.
(69) Janzen, E. G.; Evans, C. A.; Nishi, Y. *J. Am. Chem. Soc.* **1972**, *94*, 8236.
(70) Sueishi, Y.; Yoshioka, C.; Olea-Azar, C.; Reinke, L. A.; Kotake, Y. *Bull. Chem. Soc. Jpn.* **2002**, *75*, 2043.
(71) Taniguchi, H.; Madden, K. P. *J. Am. Chem. Soc.* **1999**, *121*, 11875.
(72) Liu, Y.-P.; Wang, L.-F.; Nie, Z.; Ji, Y.-Q.; Liu, Y.; Liu, K.-J.; Tian, Q. *J. Org. Chem.* **2006**, *71*, 7753.
(73) Janzen, E. G.; Evans, C. A. *J. Am. Chem. Soc.* **1973**, *95*, 8205.

JP804929D